Title	Directional far-field response of a spherical nanoantenna
Author(s)	Liu, YG; Li, Y; Sha, WEI
Citation	Optics Letters, 2011, v. 36 n. 11, p. 2146-2148
Issued Date	2011
URL	http://hdl.handle.net/10722/137299
Rights	Creative Commons: Attribution 3.0 Hong Kong License

Directional far-field response of a spherical nanoantenna

Yang G. Liu,[1] Yan Li,[1,2] and Wei E. I. Sha[1,*]

[1]*Department of Electrical and Electronic Engineering, The University of Hong Kong, Pokfulam Road, Hong Kong, China*

[2]*Department of Microwave Engineering, University of Electronic Science and Technology of China, Chengdu, 611731, China*

*Corresponding author: wsha@eee.hku.hk

We study the directional far-field response of a spherical nanoantenna via engineering the plasmonic nanosphere's distance, size, and material. A unified pattern synthesis approach based on the T-matrix method and the particle swarm optimization is proposed for the directional beamforming of the nanoantenna. The angular response of the directional nanoantenna is very sensitive to the material change but is immunized to the random error of the spatial position of each particle. The physical origin of the high directionality is attributed to the coherent near-field distribution with large correlation length. This work provides the fundamental theory and physics for future nanoantenna design.   © 2011 Optical Society of America

OCIS codes: 350.5610, 350.5030, 350.4238, 030.1640.

The metallic nanoantenna (NA) [1] is an emerging concept and technology for extreme light concentration and manipulation. Exploiting the unprecedented ability of metallic nanoparticles and nanostructures, the plasmonic antennas can convert electromagnetic radiation into concentrated and engineered field distributions. The most successful functionality of the NA includes fluorescence enhancement, surface-enhanced Raman spectroscopy, dark field microscopy, and biosensing [2–5]. The ability to tune the plasmonic resonance over a broadband or wide angle via the nanoparticle size, shape, position, and material also strongly promotes the revolutionary design of various optical devices [6].

The pattern synthesis of NAs is fundamentally important for optical beam shaping and engineered far-field scattering. Previously, the design and synthesis of NAs borrowed the idea from their radio frequency counterparts involving dipole, loop, and Yagi–Uda antennas [7–11]. In this Letter, we propose a unified pattern synthesis method for manipulating the far-field response of a spherical NA. The engineered spherical NA can redirect the incident light into highly directional far-field radiation via tuning the position, size, and material of the nanospheres. According to our investigation, the directional NA is very sensitive to material change but is immunized to the random error of the spatial distribution of the nanospheres. Particularly, we offer a deep physical insight for understanding the high directionality, which is attributed to the coherent near-field distribution with large correlation length.

Figure 1 shows the schematic design for the spherical NA. We optimize the far-field response of well-separated Ag or Au nanospheres of diameter $D \ll \lambda$, where λ is the incident wavelength. The complex refractive index of Ag and Au can be expressed by the Brendel–Bormann model [12]. The incident light propagates along the $-y$ direction and the E field is polarized along the z direction. Here each nanosphere is essentially a dipole emitter, and the engineered spatial distribution of the nanospheres can yield a constructive interference pattern in the far-field region. First, the far-field scattered field of a single nanosphere can be represented by the leading-term approximation of the T-matrix method, i.e.,

$$\mathbf{E}^s = -T_1^{(N)}\frac{3e^{ikr}}{2ikr}\sin\theta\hat{\theta} = f(\theta)\hat{\theta}, \tag{1}$$

where θ is the spherical angle with respect to the z axis, k is the wavenumber of the incident light, and $T_1^{(N)}$ is the leading-term T-matrix coefficient that can be found in [13]. Then, the far-field interference pattern of the N dipole emitters can be expressed as

$$E(\theta,\phi) = f(\theta)\sum_{n=1}^{N} e^{ik(-S_n)}, \tag{2}$$

where

$$S_n = x_n\sin\theta\cos\phi + y_n\sin\theta\sin\phi + z_n\cos\theta \tag{3}$$

and (x_n, y_n, z_n) is the coordinate of the center of the nth nanosphere. Because of the spatial spread of the nanosphere cluster, $-S_n$ is the phase shift that relates to the scattered light propagation. It should be mentioned that another phase shift x_n must be added for the excitation delay when the incident light propagates along the x direction. Compared with the single nanosphere, optimization via the additional phase shifts provides the self-phase control of the optical NA array and is the mathematical origin of the directional far-field response. Finally, we employ the particle swarm optimization (PSO) algorithm [14], which is an iterative population-based
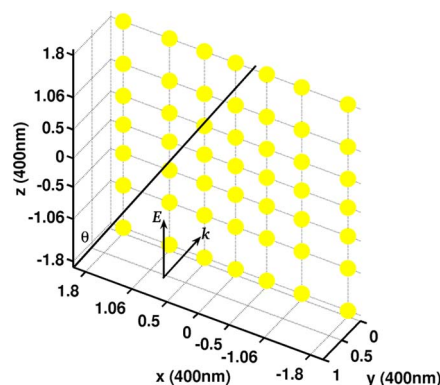

Fig. 1.   (Color online) Schematic design for the spherical NA. The wavelength of the incident light is 400 nm, and the diameter of each nanosphere is 15 nm.

stochastic technique, to achieve the desired far-field radiation pattern with high directionality and low side lobes. The optimization function is given by

$$\min \max |E(\theta, \phi)|$$
$$\text{subject to} \{|\theta - \theta_0| > w_\theta, |\phi - \phi_0| > w_\phi\}, \qquad (4)$$

where θ_0 and ϕ_0 denote the beam direction, and w_θ and w_ϕ control the beam width. In particular, the PSO algorithm can be easily extended to other nonspherical NAs if the far-field response of individual particle is known.

Figure 2(a) shows the maximum error of the angular response of a metallic nanosphere as a function of its diameter. The dipole approximation breaks down when the diameter of the nanosphere is larger than 100 nm. After that, the dipole plasmon resonance (PR) is reduced, and Mie resonance becomes more significant. Moreover, the "breakdown" diameter of the Ag nanosphere is larger than that of the Au nanosphere. It is because Ag has longer skin depth and light can penetrate it more easily for the dipole PR. Figure 2(b) illustrates the far-field scattering intensity of the directional NA as a function of the nanosphere diameter. The scattering intensity increases proportional to D^6 for small spheres, where Rayleigh scattering dominates the plasmonic spheres. As the diameter increases, Mie scattering dominates, and the growth rate of the intensity slows down. Figure 2(c) shows the optimized far-field pattern of the NA that is composed of Au nanospheres arranged in a line. We introduce the random error for each sphere's position, which always exists in the lithography process if the spherical NA is fabricated onto a substrate. Amazingly, the far-field response almost remains unchanged, and
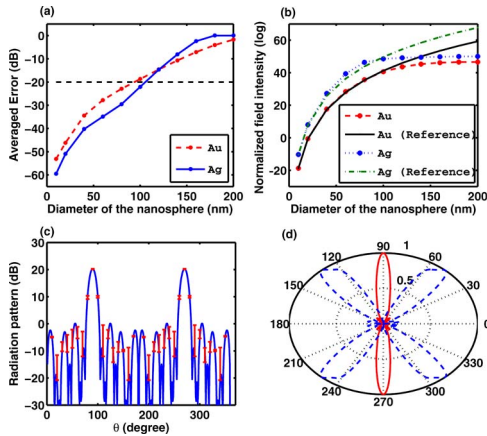

Fig. 2. (Color online) (a) Normalized angular response of a metallic nanosphere compared to that of the dipole emitter $\sin\theta$. The maximum error is drawn as a function of the nanosphere diameter. The dashed curve denotes the error $\delta = 1\%$. (b) Far-field scattering intensity of the directional NA as a function of the diameter of each nanosphere. The reference curves are calculated by using the Rayleigh approximation. (c) Uncertainty of the radiation pattern after introducing the random error of the spatial distribution of nanospheres. The red error bar indicates the standard deviation of the pattern. The space shift range from the center of each nanosphere is larger than their diameters. (d) Changed radiation pattern after replacing one of Au nanospheres by the Ag nanosphere. The red solid curve and the blue dashed curve represent the original radiation pattern and the changed radiation pattern, respectively.

the main deviations are located at the side lobes. The feature results from the cancellation of the random phase introduced by the nanospheres, and the equivalent phase center of each nanosphere still remains at the unperturbed position. Then, we replace one of Au nanospheres by the Ag nanosphere and recalculate the pattern. The drastic change of the radiation pattern can be seen in Fig. 2(d). The sensitive change is induced by the different scattering amplitude between Ag and Au nanospheres. This sensitive property can promote the potential applications in plasmonic sensing.

Figure 3(b) shows the three-dimensional highly directional far-field response of the optimized NA that is composed of Au nanospheres arranged on a plane as shown in Fig. 1. For unveiling the physical origin of the high directionality, we employ a reference spherical NA that has low directionality as shown in Fig. 3(a). First, we investigate the near-field distribution on a planar surface slightly above the two spherical NAs. The near-field distribution on the surface produces an equivalent source radiating the scattered energy into the far-field region. The planar surface with the equivalent source can be regarded as the aperture of the NAs. According to the Collett–Wolf equivalent theorem [15], the far-field radiant intensity and the spectral degree of coherence in the source plane are related by the Fourier transform. Here we extend the theorem to its vectorial form, i.e.,

$$\mathbf{E}(\mathbf{k}, \omega)\mathbf{E}^*(\mathbf{k}, \omega) = C(\hat{\theta}\hat{\theta} + \hat{\phi}\hat{\phi}) \cdot \bar{\mathbf{W}}(\mathbf{k}) \cdot (\hat{\theta}\hat{\theta} + \hat{\phi}\hat{\phi})$$

$$\bar{\mathbf{W}}(\mathbf{k}) = \int \langle \mathbf{J}(\mathbf{r}' + \mathbf{r}'', \omega) \mathbf{J}^*(\mathbf{r}', \omega) \rangle$$
$$\times \exp(-i\mathbf{k} \cdot \mathbf{r}'') d\mathbf{r}'', \qquad (5)$$

where $\mathbf{r} \to \infty$ and $\mathbf{r}'$ are the far-field observation point and the near-field source point, respectively, $C = \omega^2\mu^2/(16\pi^2 r^2)$, $\mathbf{k}$ is the wave vector, and $\mathbf{J}$ is the equivalent current source. If only J_z component exists, we have

$$|E_\theta(\mathbf{k}, \omega)|^2 = C\sin^2\theta \int \langle J_z(\mathbf{r}' + \mathbf{r}'', \omega), J_z^*(\mathbf{r}', \omega) \rangle$$
$$\times \exp(-i\mathbf{k} \cdot \mathbf{r}'') d\mathbf{r}''. \qquad (6)$$

From the theorems, the near-field coherence with large correlation length will result in high directionality of the far-field profile with small angular aperture. As illustrated in Figs. 3(d) and 3(c), the spatial correlation function of the directional NA decays much slower from the center than that of the reference NA. Hence, the directional NA has larger spatial correlation length of the near field. In view of the nonideal fabrication process again, the spatial position of each particle will be perturbed. As a result, the near-field distribution on the equivalent source plane is essentially a random process. The dimensions of the source plane are large compared with the spectral correlation length, and the directional NA has slowly varying near-field distributions. Hence, the equivalent source is assumed to be a quasi-homogeneous source [15]. With the help of the Wiener–Khintchine theorem [16], Eq. (5) can be a universal theorem for both the deterministic and random sources. For the random source, the left side of Eq. (5) becomes the spectral power
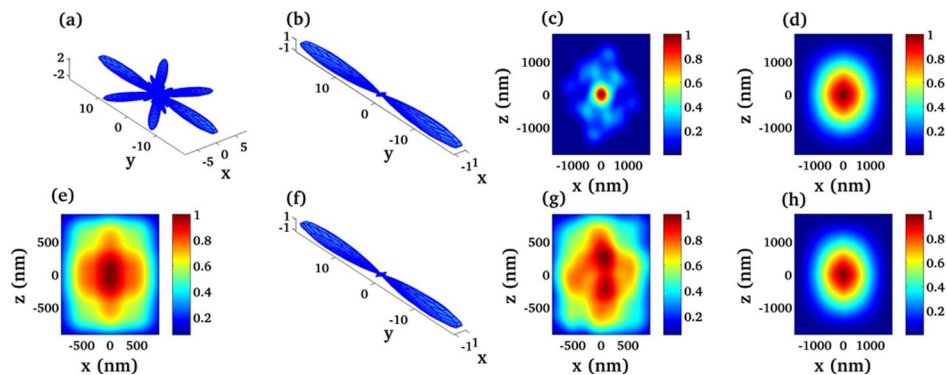
Fig. 3.   (Color online) (a), (f), and (b) Radiation patterns of the reference NA and the optimized ones with and without random fabrication errors, respectively; (c), (h), and (d) spatial correlation functions of the E_z components for the reference NA and the optimized ones with and without random fabrication errors, respectively; (g), (e) near-field intensities of the optimized NAs with and without random fabrication errors, respectively.

density $\langle \mathbf{E}(\mathbf{k}, \omega)\mathbf{E}^*(\mathbf{k}, \omega)\rangle/A$, where $A \to \infty$ is the area of source plane. Because of the random fabrication errors, the perturbed near field shown in Fig. 3(g) demonstrates significant differences from the unperturbed one shown in Fig. 3(e). However, their radiation patterns [Figs. 3(b) and 3(f)] and correlation functions [Figs. 3(d) and 3(h)] are almost the same. The above results show that an NA producing a spatially coherent equivalent source with large correlation length has a directional far-field response. Hence, the far-field radiation pattern of the NA can be engineered by controlling the near-field coherence properties.

In conclusion, we investigate the directional far-field response of a spherical NA and unveil the mathematical and physical origins of the high directionality, which are the additional phase shifts by the nanosphere cluster and the coherent near-field distribution, respectively. The far-field pattern of the optimized NA is sensitive to the material change but is immunized to the random error of the spatial position of each nanosphere. The work offers the fundamental theory and physics for future NA design.

References

1. S. J. Oldenburg, G. D. Hale, J. B. Jackson, and N. J. Halas, Appl. Phys. Lett. **75**, 1063 (1999).
2. T. Kalkbrenner, U. Hakanson, A. Schadle, S. Burger, C. Henkel, and V. Sandoghdar, Phys. Rev. Lett. **95**, 200801 (2005).
3. S. Kuhn, U. Hakanson, L. Rogobete, and V. Sandoghdar, Phys. Rev. Lett. **97**, 017402 (2006).
4. A. Kinkhabwala, Z. F. Yu, S. H. Fan, Y. Avlasevich, K. Mullen, and W. E. Moerner, Nat. Photon. **3**, 654 (2009).
5. L. Novotny and N. van Hulst, Nat. Photon. **5**, 83 (2011).
6. H. A. Atwater and A. Polman, Nat. Mater. **9**, 205 (2010).
7. P. Muhlschlegel, H. J. Eisler, O. J. F. Martin, B. Hecht, and D. W. Pohl, Science **308**, 1607 (2005).
8. J. J. Li, A. Salandrino, and N. Engheta, Phys. Rev. B **76**, 245403 (2007).
9. A. Alu and N. Engheta, Nat. Photon. **2**, 307 (2008).
10. T. H. Taminiau, F. D. Stefani, and N. F. van Hulst, Opt. Express **16**, 10858 (2008).
11. A. Ahmadi and H. Mosallaei, Opt. Lett. **35**, 3706 (2010).
12. A. D. Rakic, A. B. Djurisic, J. M. Elazar, and M. L. Majewski, Appl. Opt. **37**, 5271 (1998).
13. L. Tsang, J. A. Kong, and K. H. Ding, *Scattering of Electromagnetic Waves: Theories and Applications* (Wiley, 2000).
14. J. Robinson and Y. Rahmat-Samii, IEEE Trans. Antennas Propag. **52**, 397 (2004).
15. W. H. Carter and E. Wolf, J. Opt. Soc. Am. **67**, 785 (1977).
16. J. W. Goodman, *Statistical Optics* (Wiley, 2000).